ZURICH, SWITZERLAND
6 - 10 OCTOBER 2025

EUROPEAN GEOTHERMAL CONGRESS 2025

Feasibility Assessment of Aquifer Thermal Energy Storage: A Case Study in Riva del Garda, Italy

Masoud Manafi[1,*], Vaiva Cypaite[2], Ehsan Ranaee[3], Fabio Inzoli[3], Rodolfo Perego[4], Bas Godschalk[5], Nico Franco Pinto[6], Peter Oerlemans[6], Frederik Jansen[6], Diego Viesi[1].

[1] Center for Sustainable Energy, Fondazione Bruno Kessler (FBK), via Sommarive 18, 38123 Povo (TN), Italy

[2] Seequent, The Bentley Surface Company, 20 Moorhouse Avenue, Christchurch, New Zealand

[3] Dipartimento di Energia, Politecnico di Milano, Via Lambruschini 4, 20156 Milan, Italy

[4] Institute of Earth Sciences, University of Applied Sciences and Arts of southern Switzerland SUPSI - Campus Mendrisio, Via Flora Ruchat Roncati 15 CH, 6850, Mendrisio, Switzerland

[5] DTESS, Zomertalinghof 29, 8043 JW Zwolle, the Netherlands

[6] IF Technology, Velperweg 35, 6824 BE Arnhem, the Netherlands

[*] mmanafi@fbk.eu

Keywords: Aquifer Thermal Energy Storage (ATES), thermal recovery efficiency, hydrogeological characteristics, numerical modeling.

ABSTRACT

Aquifer Thermal Energy Storage (ATES) systems have emerged as a promising technology for balancing seasonal variations in energy supply and demand, particularly in heating and cooling applications. By acting as seasonal buffers, ATES systems in larger scales can contribute to the stability of heating networks and offer flexibility in the electricity market through power-to-heat technologies such as heat pumps and electric boilers, thereby facilitating the integration of renewable energy sources. However, their successful deployment depends on a comprehensive understanding of local subsurface conditions, especially hydrogeological characteristics. Present study investigates the feasibility of ATES systems in a shallow confined aquifer (less than 200 *m* depth) in Riva del Garda, Italy. A site-specific numerical model was developed to assess system performance with a focus on recovery efficiency including a sensitivity analysis to explore the influence of three key parameters: (i) variability in hydraulic conductivity, (ii) strength of hydraulic gradients, and (iii) temperature magnitude of injected water for storage. Numerical simulations were conducted in the FEFLOW© software environment, enabling a robust evaluation of thermal behavior under multiple operational conditions. Further developments using the Volsung toolkit aims to refine the simulation model and explore the impact of subsurface variability in greater details. The obtained results confirm potential of ATES systems as a viable solution in line with the targets of decarbonizing large heating networks in Riva del Garda, Italy. Our findings emphasize the significant importance of hydraulic gradient, hydraulic conductivity, well spacing, and injection water temperature in shaping thermal recovery efficiency and overall system effectiveness.

1. INTRODUCTION

The heating and cooling sector in Europe accounts for nearly 50% of the total final energy consumption and remains predominantly reliant on fossil fuels (Heat Roadmap Europe, 2017). Consequently, rapid decarbonization of this energy sector is essential to meet the EU climate neutrality targets by 2050 (European Commission, 2020). Advancing toward low-carbon heat sources such as geothermal energy, biomass, solar thermal, and waste heat requires storage systems that can buffer the variability of supply and demand, particularly in response to seasonal fluctuations (Guglielmetti et al., 2019). Achieving those decarbonization goals requires accelerating the adoption of renewable energy sources (RES) and innovative technologies. Among the key solutions is district heating and cooling (DHC), which enables (i) the integration of RES and waste heat sources, (ii) supports sector coupling, and (iii) enhances flexibility in supply and demand of the electricity market. According to Article 26 of the European Energy Efficiency Directive (Directive EU 2023/1791), the integration of RES and waste heat into the DHC systems is required to progressively increase. This directive stipulates progressively more stringent thresholds for the inclusion of RES, waste heat, or high-efficiency cogenerated heat, aiming to enhance the sustainability and operational efficiency of DHC networks. Given the inherent fluctuations in the availability of RES and waste heat, as well as the variability in thermal energy demand—driven by both

daily and seasonal cycles—the achievement of these targets necessitates the incorporation of large-scale thermal energy storage systems. These systems are crucial for mitigating temporal mismatches between supply and demand, enhancing system flexibility, and facilitating the transition towards a decarbonized heating and cooling infrastructure.

Underground Thermal Energy Storage (UTES) technologies, particularly ATES systems, have recently emerged as viable solutions for integration with DHC networks. These subsurface systems offer sustainable and environmentally friendly options to reduce greenhouse gas emissions while addressing growing energy demands. In seasonal applications, they provide heating in winter and cooling in summer. In recent years, heat storage using ATES systems has gained interest. A typical ATES setup includes extraction and injection wells, heat exchangers, pumps, and a heat source/demand (**Fig. 1**). During summer, groundwater is extracted from a tepid well, heated via a heat exchanger using RES, waste heat, or surplus heat, and then injected into the aquifer through a warm/hot well for storage. In winter, the stored warm/hot water is recovered and used for heating before being returned to the aquifer through the tepid well.

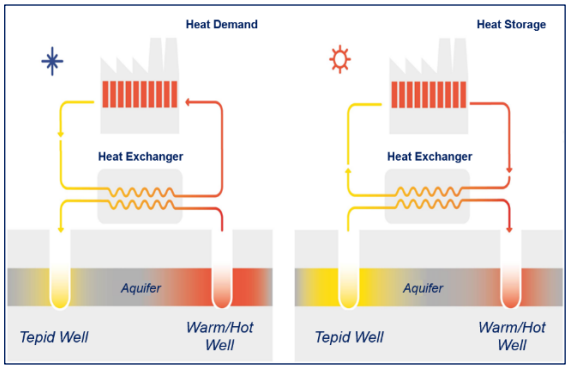

Figure 1. Simple schematic of an ATES system for seasonal operation (adopted from dtess.com).

Modeling studies of a single ATES well show that thermal recovery is always lower than 100% as a result of heat loss due to regional groundwater flow (Kangas and Lund, 1994) and heat conduction (Chevalier and Banton, 1999; Doughty et al., 1982; Sauty et al., 1982a). One of the key aspects is the design and placement of wells, which have been comprehensively investigated with respect to hydrogeological conditions (Bloemendal and Hartog, 2018; Doughty et al., 1982; NVOE, 2006). Concerning the role of hydrogeological traits, Manafi (2022) showed that the influence of capillary pressure and evapotranspiration on thermal recovery can be negligible. The storage volume and groundwater flow are also key parameters in the design of ATES systems (Bloemendal and Olsthoorn, 2018; Doughty et al., 1982). For ATES systems operating at higher temperatures, the relative potential for buoyant flow—a key process dependent on injection temperature, vertical permeability, aquifer thickness, and thermal parameters—may be assessed through Rayleigh number analysis (Krol et al., 2014). Schout et al. (2014) presented a correlation between a modified Rayleigh number and HT-ATES, while Sheldon et al. (2021) extended this work to a broader range of hydrogeological and operational conditions, although this approach overlooks the impact of ambient groundwater flow. Variation in vertical hydraulic conductivity has also been shown to be an important parameter for HT-ATES systems (Heldt, 2024). However, in areas like the one examined in the present study with limited number of field measurements and subsurface information, it is crucial to numerically assess the response of a single doublet ATES system under varying hydrogeological conditions.

The present research, conducted as part of the USES4HEAT project (HORIZON-CL5-2023-D3-01-14), aims to investigate the feasibility of implementing ATES in Riva del Garda, Italy. While the successful deployment of such a system typically requires consideration of mechanical, reservoir, and geophysical aspects, this study focuses primarily on the subsurface modeling and hydrogeological analysis needed to assess ATES potential in the area. Moreover, a sensitivity analysis was performed on the hydrogeological properties of the reservoir for three different categories of ATES system temperature conditions: (a) low-temperature water injection (LT-ATES, ~25 $°C$), (b) medium-temperature water injection (MT-ATES, ~40 $°C$), and (c) high-temperature water injection (HT-ATES, ~80 $°C$).

2. STUDY AREA: RIVA DEL GARDA, ITALY

2.1. Geological Framework

Some previous studies have been conducted to evaluate the sedimentary history of the area (Felber et al., 1998; GeoAlp, 2024), providing a geological model for the infill of the Basso Sarca Valley. These findings are supported by geophysical investigations (Benvenuti et al., 1970; Felber et al., 1998) and stratigraphic data obtained from deep wells located in the Riva del Garda and Arco regions. The expected stratigraphic succession in the study area is as follows (see **Fig. 2**):

- Fill soil (not illustrated in the figure): Composed of coarse gravels mixed with anthropogenic materials, with an estimated thickness of approximately 2–3 m.
- Delta fan and alluvial deposits: Comprised of coarse gravels and sands, these unconsolidated deposits host a rich aquifer and reach a thickness of around 50 m. Locally, conglomerate crusts may form near the oscillation range of the groundwater table, which in this area fluctuates around 5 meters below the surface.
- Lacustrine deposits: Alternating sandy silts and clays, with an estimated thickness of about 85 m.
- Glacial and fluvioglacial deposits: Fine and silty sands and gravels embedded in a silty-clayey matrix, interspersed with gravelly horizons. This layer also contains aquifers and is the target for the ATES study. Its thickness is presumed to be around 25 m.

- River deposits: Consist of gravels, sands, and debris-flow blocks along the sides of the valley. They are likely present along the ancient pre-glacial valley axis and are weakly cemented. These deposits contain aquifers and have a presumed thickness of approximately 20 *m*.
- Bedrock: Composed of fractured limestone and dolomite, with its upper boundary occurring at an approximate depth of 180 *m*.

2.2. Hydrogeological Framework

The Basso Sarca Valley features a multilayered aquifer system, where individual aquifers are separated by silty clay layers with low or negligible permeability. The unconfined aquifer stretches from Lake Garda to Dro is highly transmissive, which has been extensively studied and utilized in literature.

Recharge sources include inflows from karstic carbonate mountains, sub-alveolus seepage from the Sarca River, lateral stream inflow, rainfall infiltration, and irrigation. **Figure 3** presents a hydrogeological map showing the shallow groundwater table and flow directions between Arco and Riva del Garda. A notable cone of depression is visible, caused by groundwater extraction from Cartiere del Gada wells. Piezometric data collected over more than 50 years indicate minimal long-term variations in water levels, which remain stable at approximately 66 *m* above sea level near Riva del Garda. However, localized drawdowns are evident around industrial extraction zones.

As for the deep confined aquifer located beneath the lacustrine deposits, data remains limited. Available insights stem primarily from boreholes such as the San Giorgio well, where the confined aquifer's static level is found to be close to that of the phreatic aquifer. Moreover, based on pumping test data from the Du Lac et Du Parc Grand Resort, and assuming an aquifer thickness of 25 *m*, the estimated transmissivity yields a range of hydraulic conductivity values between 5×10^{-5} and 6.2×10^{-5} *m/s*. This estimate aligns with sediments composed of fine and silty sands but must be treated with caution. Pumping tests exhibit irregular patterns, suggesting potential interaction with multiple aquifers and it is assumed that the aquifers are connected with each other in some points with the same hydraulic gradients $i = 0.0026$ and direction from the San Giorgio to the Lake Garda. No consistent records of temperature or groundwater levels exist for the confined aquifer, limiting further assessment, particularly with regard to connectivity with Lake Garda.

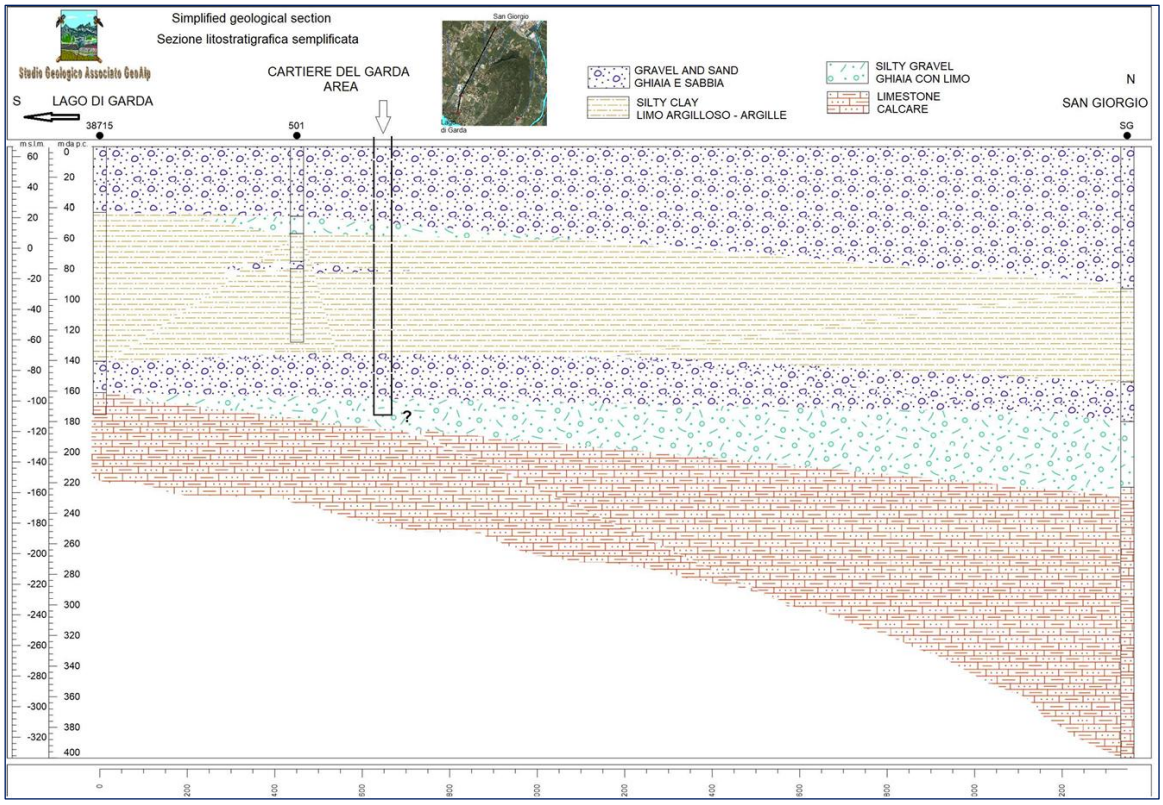

Figure 2. Interpreted stratigraphic cross-section between San Giorgio and Lake Garda (GeoAlp, 2024).

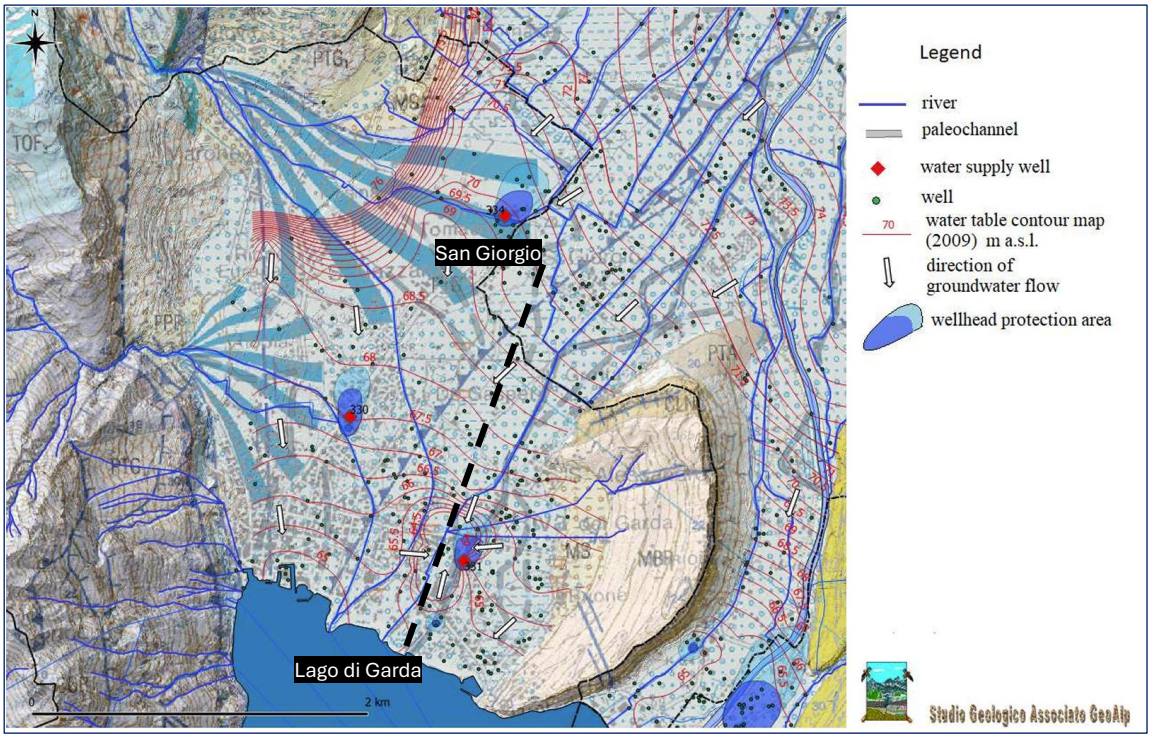

Figure 3. Hydrogeological map of the study area (GeoAlp, 2024).

2.3. Identification of the Heat Source for Storage

Figure 4 illustrates heat supply records for the DHN in Riva del Garda in 2023. The main energy source is an economizer installed at the outlet of the Heat Recovery Steam Generator (HRSG) in the combined heat and power (CHP) plant. The economizer provides a daily average thermal output potential of approximately 180 *MWh*, a portion of which remains unused during the summer months. Peak demand during winter is satisfied by a heat pump and other existing components in the plant (i.e., steam/water heat exchangers and auxiliary natural gas boilers). For the ATES system, the economizer serves as the primary source for thermal charging. To estimate the amount of recoverable waste heat available during summer operation, hourly supply data were analyzed. Between mid-April and mid-October, the unused waste heat potential from the HRSG is estimated at approximately 7.5 *GWh*, corresponding to an output power ranging between 1.5 and 3 *MW* during operational hours. The waste heat is available within a temperature range of 65–90 °*C*. The total energy allocated for storage, assuming a constant storage volume in each ATES scenario, is as follows:

- LT-ATES (~25 °*C*): 1.6 *GWh*
- MT-ATES (~40 °*C*): 3.75 *GWh*
- HT-ATES (~80 °*C*): 9.5 *GWh*

Note that for the HT-ATES, the additional heat for charging comes from one of the steam/water heat exchangers, which has a limited amount of recovery potential during the summer.

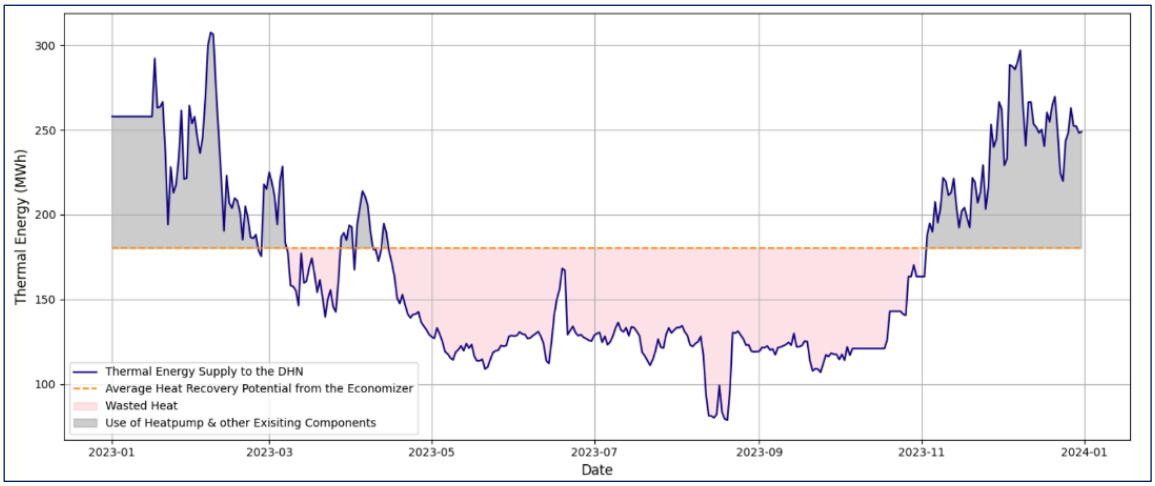

Figure 4. Daily thermal energy supply profile for district heating network (dark blue line) for Riva del Garda in 2023, highlighting the economizer recovery potential (orange dashed line), available excess heat during the summertime (pink area), and the utilization of other components to meet the peak demand during wintertime (gray area).

3. MATERIALS AND METHODS

3.1. Simulation Model Setup

Simulation conducted in FEFLOW software environment. The analysis incorporates Richards' equation (1931) for variably saturated porous media, along with transient-state heat transport, accounting for temperature-dependent fluid density and viscosity. The unsaturated conditions were modeled using the van Genuchten (1985) formulation, with residual saturation (S_r) = 0.05, and empirical parameters α = 0.1, and n = 1.964 which are suited to the case study aquifer. Numerical models encompass a horizontal area 1×1 km^2 (**Fig. 5**) with four vertical layers (**Table 3**) including aquitard (the lacustrine deposits with clay and silty sands), confined aquifer (the glacial and fluvioglacial deposits with fine and silty sands), river deposits (fractured matrix with gravel and silty sands), and bedrock (limestone and dolomites).

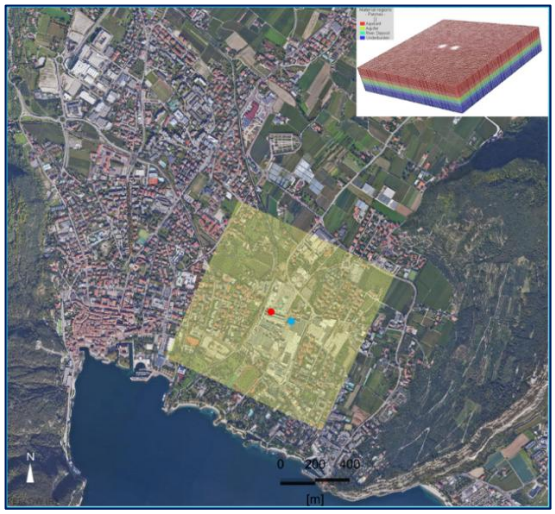

Figure 5. Top view of the location of interest in Riva del Garda, highlighting the model area in yellow and the locations of the wells.

Tables 1 and **2** present the hydrogeological and thermal properties adopted for all simulation scenarios. In the absence of site-specific measurements, it was assumed that each geological formation has homogeneous properties across the study area, as detailed hydrogeological data were interpreted from regional studies rather than direct borehole logs.

To evaluate the influence of key hydrogeological parameters, a sensitivity analysis was conducted, focusing on two major factors of: (i) hydraulic conductivity and (ii) hydraulic gradient. **Table 3** provides the range of values assigned for those parameters, covering different ATES categories (LT-, MT-, and HT-). For each parameter, three distinct values were considered: a baseline, a fivefold increase, and a fivefold decrease in hydraulic gradient, along with a one-order-of-magnitude variation in hydraulic conductivity. In total, 27 simulation model scenarios were simulated for this analysis.

It is important to note that this study exclusively examined the effects of those two hydrogeological parameters, without modifying the thermophysical properties of the geological layers.

Table 2. General configuration parameters adopted for numerical simulation.

Parameter	Value *[unit]*
Cold well Injection Temperature	14 *[°C]*
Injection/Production flow rate	1037 *[m^3/day]*
Heat Storage/Recovery Period	120 *[day]*
Storage Standstill	60 *[day]*
Total Simulation Time	3600 *[day]*
Well Spacing	130 *[m]*
Borehole Radius	175 *[mm]*
Well Screen Length	25 *[m]*
Groundwater Average Temperature	14 *[°C]*

Table 3. Parameters values considered for the sensitivity analysis, with their units. L, M, and H indicate low, medium, and high values, respectively.

Properties *[unit]*	LT-ATES (T^L)	MT-ATES (T^M)	HT-ATES (T^H)
Hydraulic Gradient *[10^{-3}]*	0.52 (i^L) 2.6 (i^M) 13 (i^H)	0.52 (i^L) 2.6 (i^M) 13 (i^H)	0.52 (i^L) 2.6 (i^M) 13 (i^H)
Hydraulic Conductivity *[10^{-5} m/s]*	0.56 (k^L) 5.6 (k^M) 56 (k^H)	0.56 (k^L) 5.6 (k^M) 56 (k^H)	0.56 (k^L) 5.6 (k^M) 56 (k^H)

Table 1. Hydrogeological and thermal properties of the layers adopted in the simulation models.

Rock/ Property	Top surface elevation *[m a.s.l.]*	Thickness *[m]*	Horizontal hydraulic conductivity *[m/s]*	Vertical hydraulic conductivity *[m/s]*	Porosity *[]*	Volumetric heat capacity of solid *[J/m^3/K]*	Thermal Conductivity of solid *[J/m/s/K]*
Aquitard	20	85	1.2×10^{-9}	1.2×10^{-10}	0.12	2.4×10^{6}	1.2
Storage Aquifer	-65	25	5.6×10^{-5}	5.6×10^{-6}	0.19	3×10^{6}	2
River Deposits	-90	20	10^{-6}	10^{-6}	0.2	2.5×10^{6}	2.25
Bedrock	-110	70	10^{-9}	10^{-10}	0.1	2.34×10^{6}	2.5

3.2. Well Placement

Several site-specific constraints were considered in the decision-making process for the placement of the ATES wells:

- Geographical constraints, including nearby rivers and subsurface infrastructure
- Safety and interference with existing shallow wells, requiring a sufficient buffer distance
- Operational feasibility, prioritizing locations that are accessible for drilling equipment and as close as possible to the power plant, to minimize costs associated with electrical and hydraulic connections

The optimal distance between injection and extraction wells was determined using the thermal radius approach proposed by Doughty et al. (1982). The thermal radius (R_{th}) is given by:

$$R_{th} \triangleq \sqrt{\frac{c_w V_{in}}{c_{aq} \pi L}} \quad [1]$$

Where c_w *[J/m³/K]* denotes the volumetric heat capacity of water, V_{in} *[m³]* is stored groundwater volume, c_{aq} *[J/m³/K]* indicates the volumetric heat capacity of the saturated aquifer, and *L [m]* represents the total screen length.

As emphasized by Regnier et al. (2022), the indicated formulation for the thermal radius does not account for thermal conduction, dispersion, vertical flow, or geological heterogeneities, and may therefore lead to simplified estimates. Drawing from Birdsell et al. (2021) and Kim et al. (2010), optimal well spacing for LT-ATES is typically within the range of 1–3 thermal radii, though this can vary depending on site-specific conditions. For heat storage applications only, Dutch standards suggest that the thermal radius can be less than 3 thermal radii (NVOE, 2006), and having a closer well distance usually increases the recovery efficiency and decreases thermal loss, but it may increase the temperature in the tepid well and thus reduce the potential for heat storage. In this study, the well distance was set at 2.5 R_{th} as per equation [1].

4. RESULTS

4.1. Wellhead Temperature Over Time

Simulations were performed for 27 model scenarios, and wellhead temperatures were recorded at both wells (i.e., warm/cold). Considering the general model with estimated hydraulic values (denoted as $i^M.k^M$) for the three types of ATES systems, the warm/hot well temperatures showed acceptable results (**Figs. 6, 7, and 8**). During the storage standstill period, the wellhead temperature dropped by approximately 1 °*C*, 2.5 °*C*, and 8 °*C* for LT-, MT-, and HT-ATES, respectively. At the end of the heat recovery period, the wellhead cut-off temperatures were recorded at 20 °*C*, 27.5 °*C*, and 45 °*C* for LT-, MT-, and HT-ATES, respectively, in the fourth storage cycle.

For the LT-ATES scenario (**Fig. 6**), results show that increasing both hydraulic conductivity and hydraulic gradient leads to a greater decline in warm wellhead temperatures over time, particularly during the storage period, indicating higher thermal losses. In the case with high hydraulic conductivity and hydraulic gradient ($i^H.k^H$), nearly all stored heat is lost due to advection and dispersion. Conversely, reducing either hydraulic gradient or/and hydraulic conductivity (e.g., $i^L.k^L$, $i^M.k^L$, $i^L.k^M$) produces only minor variations in temperature. Comparing intermediate scenarios ($i^M.k^M$, $i^M.k^H$, $i^L.k^M$, $i^H.k^M$) suggests that hydraulic conductivity has a more pronounced effect on thermal losses than the hydraulic gradient. Notably, in the scenario low with hydraulic gradient, high hydraulic conductivity ($i^L.k^H$), the wellhead temperature drops significantly, confirming the dominant role of advection in heat loss.

For MT-ATES (**Fig. 7**), the sensitivity trends are similar to LT-ATES scenarios. Lower hydraulic conductivity and hydraulic gradient values show limited impacts on wellhead temperatures. Among the comparative cases ($i^M.k^M$, $i^M.k^H$, $i^L.k^M$, $i^H.k^M$), hydraulic conductivity again appears to be the controlling factor. This is especially evident when comparing $i^H.k^M$ and $i^L.k^H$, which exhibit similar thermal responses despite differing gradients, emphasizing that conductivity governs thermal loss more strongly than gradient under these conditions.

In HT-ATES models (**Fig. 8**), even under low-gradient conditions (i^L), the wellhead temperature declines rapidly. This is attributed to buoyancy-driven flow, which becomes increasingly relevant at elevated temperatures. Comparing the $i^L.k^H$ and $i^H.k^M$ cases further confirms that higher hydraulic conductivity significantly accelerates heat loss during the storage phase. Additionally, as heat is stored at higher temperatures, the reduced water viscosity can increase effective hydraulic conductivity, potentially leading to even greater heat losses than initially anticipated. These findings underscore the importance of site-specific hydrogeological properties in determining the thermal performance of ATES systems, particularly at higher storage temperatures.

For LT-ATES and MT-ATES configurations (**Figs. 9 and 10**), the simulation results indicate no significant temperature increase at the cold well in all scenarios, suggesting that the chosen well spacing effectively mitigates thermal interference. In fact, closer well spacing could further reduce thermal losses from the warm well without substantially affecting the cold well, potentially enhancing overall system efficiency. Overall, since the water volumes are similar, it shows that MT-ATES can store more heat compared to LT-ATES.

However, in HT-ATES scenarios (**Fig. 11**), particularly under low hydraulic gradient conditions, noticeable thermal interference was observed. Warm water gradually migrated toward the cold well, raising its temperature over time and reducing the available storage potential in subsequent summer cycles. While

this temperature rise can act as a thermal barrier, reducing heat loss from the warm well, it also decreases the long-term storage capacity by limiting the effective temperature differential.

Overall, these findings highlight the delicate balance between maximizing thermal efficiency and optimizing stored heat volume, especially in geologically constrained environments, such as those studied by Fleuchaus et al. (2018) in the Netherlands. In such cases, reduced well spacing may offer both technical and economic advantages. For this study, given the limited model domain, a constrained optimization approach is recommended. In practice, determining the optimal well spacing often requires a trial-and-error process, which remains a feasible strategy under the test case conditions.

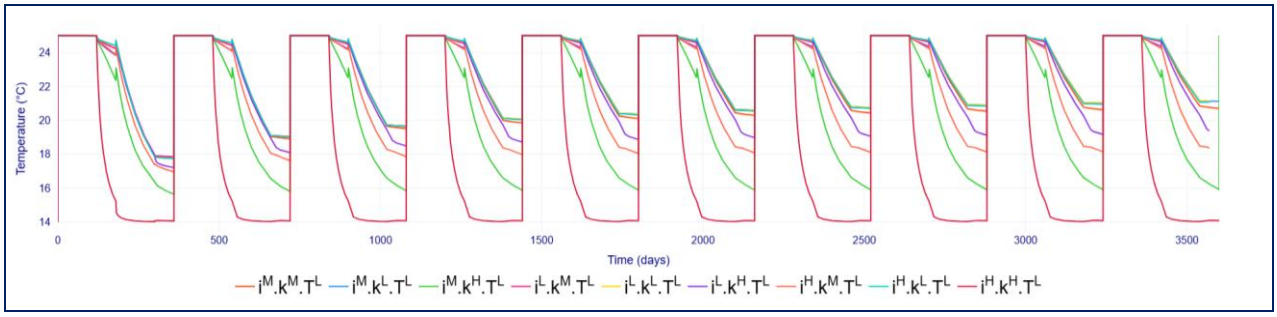

Figure 6. Temporal evolution of the warm well head temperature in the LT-ATES system over 3,600 days of simulation.

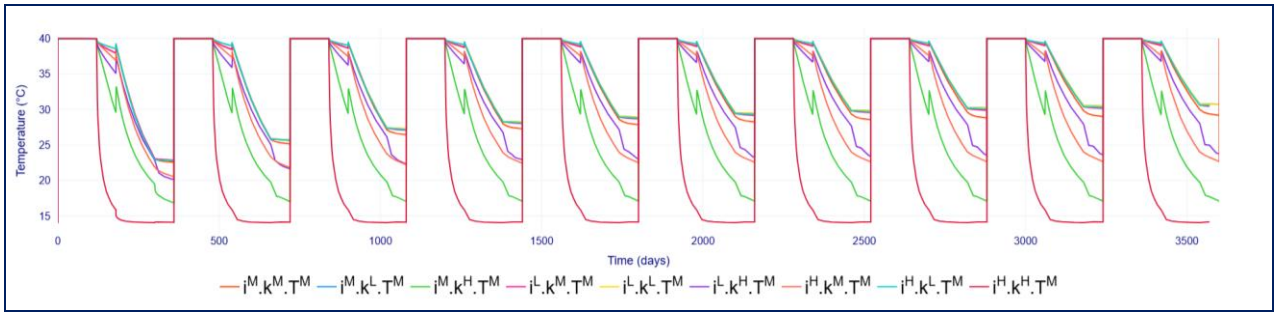

Figure 7. Temporal evolution of the warm well head temperature in the MT-ATES system over 3,600 days of simulation.

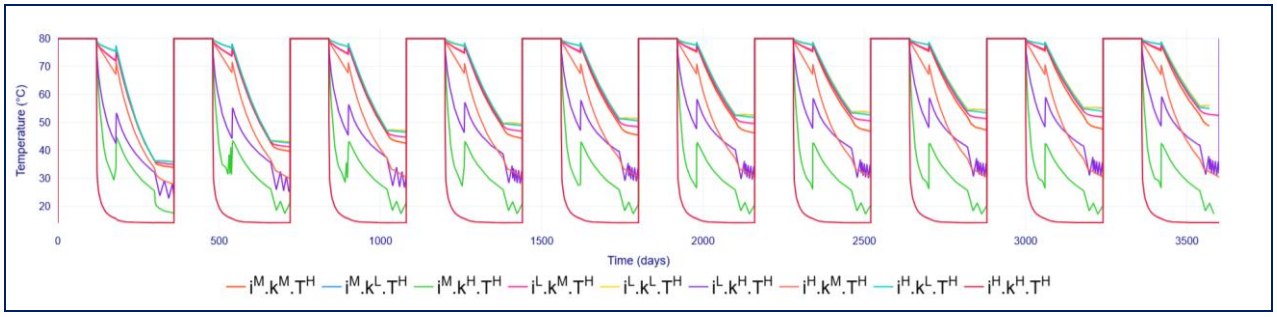

Figure 8. Temporal evolution of the hot well head temperature in the HT-ATES system over 3,600 days of simulation.

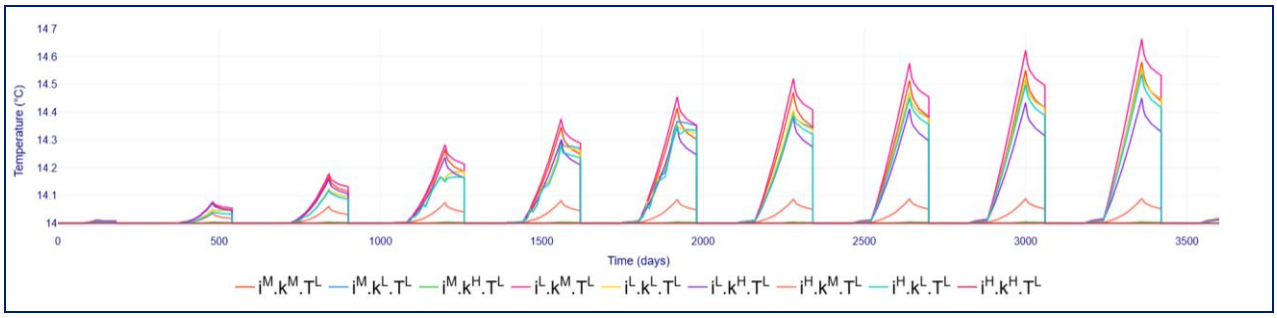

Figure 9. Temporal evolution of the cold well head temperature in the LT-ATES system over 3,600 days of simulation.

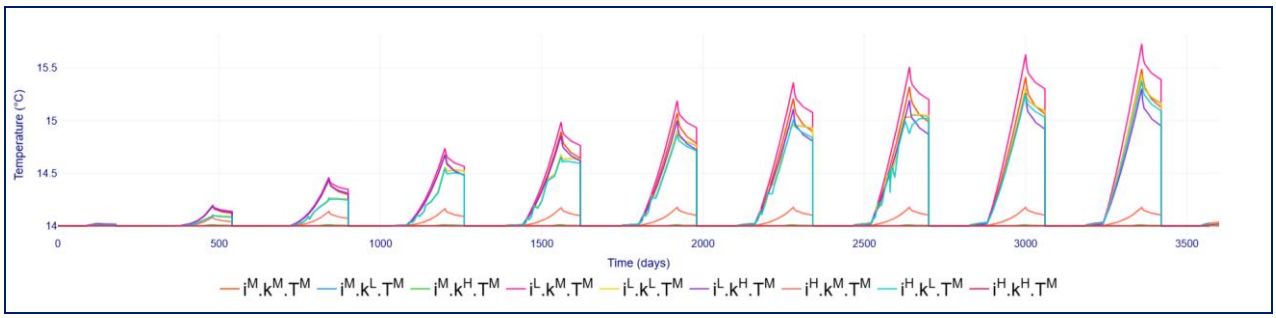

Figure 10. Temporal evolution of the cold well head temperature in the MT-ATES system over 3,600 days of simulation.

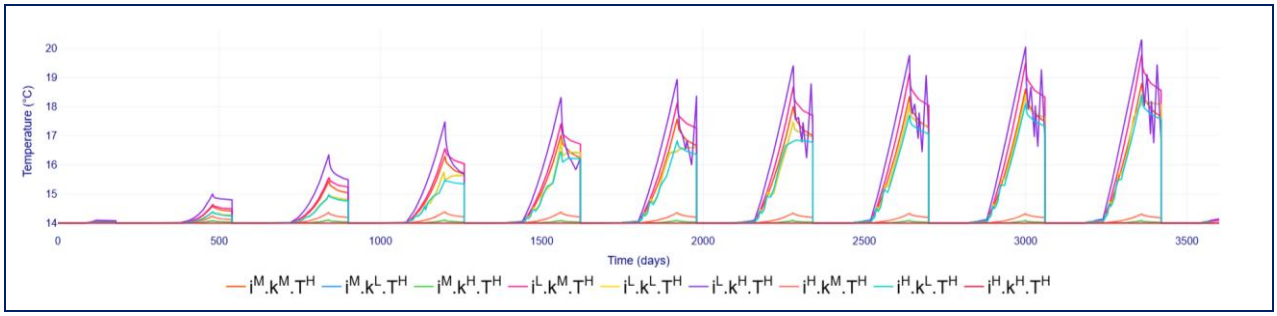

Figure 11. Temporal evolution of the cold well head temperature in the HT-ATES system over 3,600 days of simulation.

4.2. Thermal Recovery Efficiency

A widely adopted metric for evaluating ATES system performance is Thermal Recovery Efficiency (or Thermal Recovery Factor), denoted as RE_{th} defined by Sommer et al. (2013) as:

$$RE_{th} \triangleq \frac{\int_{Prod.} q_{prod}(T-T_n)dt}{\int_{Inj.} q_{inj}(T-T_n)dt} \quad [2]$$

Where T *[K]* is the wellhead temperature, T_n *[K]* the average initial undisturbed aquifer temperature over the well screen length and q_{inj} *[m^3/day]* is the injection and q_{prod} *[m^3/day]* is the production flow rates.

As illustrated in **Figures 12, 13, and 14**, thermal recovery efficiencies of up to 70% can be achieved after ten years of operation across various scenarios, aligning with the earlier discussions. Notably, reducing either the hydraulic gradient (i^L) or hydraulic conductivity (k^L) independently had little impact on recovery efficiency for all three ATES categories.

In contrast, models with higher hydraulic conductivity ($i^M.k^H$) exhibited a steady recovery efficiency of approximately 40% for LT- and MT-ATES, while the efficiency dropped significantly by 10% (RE_{th} = 30%) for HT-ATES. This trend was similarly observed in models with low gradient but high conductivity ($i^L.k^H$), where recovery efficiency decreased by approximately 20% (RE_{th} = 45%) for HT-ATES compared to the other two categories (LT- and MT-ATES).

Increasing only the hydraulic gradient ($i^H.k^M$) resulted in a modest 5% reduction in recovery efficiency (RE_{th} = 50%) for HT-ATES relative to LT- and MT-ATES. As expected, scenarios combining high gradient and high hydraulic conductivity ($i^H.k^H$) resulted in zero recovery across all three ATES configurations, as the stored heat rapidly dispersed due to enhanced groundwater flow and thermal advection.

These findings underscore the critical importance of aligning operational parameters with site-specific hydrogeological conditions to ensure long-term thermal efficiency and energy sustainability in ATES systems.

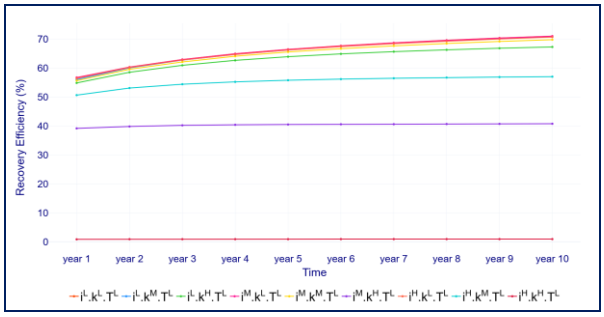

Figure 12. Warm well thermal recovery efficiency over time for the LT-ATES system.

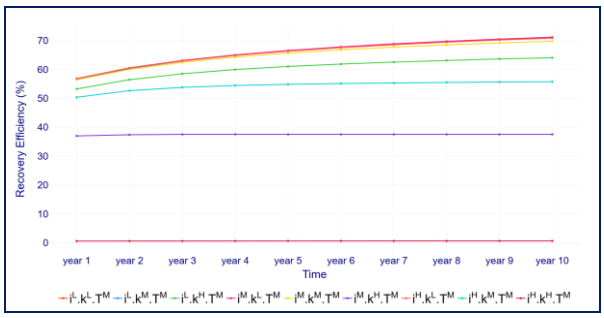

Figure 13. Warm well thermal recovery efficiency over time for the MT-ATES system.

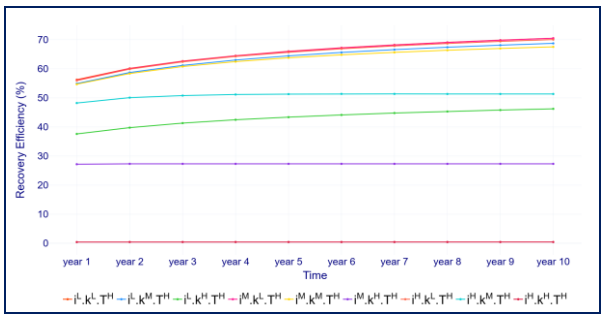

Figure 14. Hot well thermal recovery efficiency over time for the HT-ATES system.

5. CONCLUSION

This study numerically assess the feasibility and performance of an ATES system for heat storage applications using a two-well (single-doublet) configuration in the Riva del Garda region of Northern Italy, as part of the USES4HEAT project. Accounting for geological and hydrogeological characterization, combined with thermal-hydraulic simulations performed in FEFLOW, the potential for integrating seasonal thermal energy storage into the local DHN was systematically evaluated.

Obtained results for three ATES configurations—LT-ATES, MT-ATES, and HT-ATES—highlight the critical influence of hydraulic conductivity, hydraulic gradient, and injection water temperature on system performance. For systems operating with two wells, higher hydraulic conductivity and gradients significantly accelerate thermal dispersion, reducing wellhead temperatures and thermal recovery efficiency, particularly in the HT-ATES system. Buoyancy effects were also found to strongly influence performance of HT-ATES scenarios, even under low-hydraulic gradient conditions. It is important to note that these results and insights are specific to the range of parameter values used in this study, emphasizing the need for precise thermal-hydraulic modeling at elevated temperatures.

Simulation results suggest that thermal recovery efficiencies can reach values as high as 70% under favorable conditions, affirming the technical viability of ATES in the studied area, particularly for low- to medium-temperature storage systems. However, the potential for thermal interference between wells, particularly in HT-ATES scenarios, underscores the need for accurate geological data and optimized well spacing, as well as site-specific design strategies.

Despite regulatory challenges, the Riva del Garda area, supported by an available waste heat source, favorable geological conditions, and increasing energy demand, presents a promising opportunity for the successful implementation of ATES systems.

6. DISCUSSION AND NEXT STEPS

While this study primarily focused on the subsurface modeling of ATES systems, several areas for further improvement and investigation have been identified. One notable limitation is the exclusion of frictional losses and pressure drops within the wells. Although these effects are generally minor in shallow aquifer systems with vertical wells, they can become more significant in medium- to high-temperature systems. To capture the system dynamics more accurately, future studies should consider using multiphase solver software capable of accounting for complex pressure and flow behavior.

Additionally, the sensitivity analysis was performed with a focus exclusively on variations in hydraulic gradient and hydraulic conductivity. However, a more comprehensive assessment would benefit from including thermal properties such as thermal conductivity, volumetric heat capacity, and dispersivity, as these parameters can influence heat transfer and storage efficiency in ATES systems.

While heterogeneity in geological properties was not investigated in this study, further exploration of this factor is recommended, especially for HT-ATES systems. Understanding the effects of geological variability, particularly in relation to well spacing, could provide insights into optimizing system performance. A sensitivity analysis that incorporates heterogeneous rock properties may reveal opportunities to enhance storage capacity and recovery efficiency, leading to more robust and site-specific system designs.

To address those challenges, our ongoing work focuses on simulating multiphase geothermal systems. This effort aims to provide a more comprehensive approach to modeling complex subsurface behaviors, offering valuable insights as the study progresses. Future updates will incorporate these advanced modeling techniques, further refining our understanding of ATES system performance within DHNs.

REFERENCES

Heat Roadmap Europe, 2017. Heating and Cooling: Facts and Figures. The Transformation towards a Low-Carbon Heating & Cooling Sector. https://heatroadmap.eu/wpcontent/uploads/2019/03/Brochure_Heating-and-Cooling_web.pdf.

European Commission, 2020. 2050 long-term strategy. https://ec.europa.eu/clima/policies/strategies/2050_en.

Directive (EU) 2023/1791 of the European Parliament and of the Council of 13 September 2023 on energy efficiency and amending Regulation (EU) 2023/955 (recast) (Text with EEA relevance) ELI: http://data.europa.eu/eli/dir/2023/1791/oj

Guglielmetti, L., Meier, P., Driesner, T., Diamond, L. and Valley, B., 2019. Heatstore: aquifer thermal energy storage in switzerland. In SCCER-SoE Annual Conference 2019 (p. AC19_S4a_03). Swiss Competence Center for Energy Research–Supply of Electricity (SCCER-SoE).

Kangas, M. T., and P. D. Lund (1994), Modeling and simulation of aquiferstorage energy-systems, Sol. Energy, 53(3), 237–247.

Chevalier, S., and O. Banton (1999), Modelling of heat transfer with therandom walk method. Part 1. Application to thermal energy storage inporous aquifers, J. Hydrol., 222(1–4), 129–139.

Sauty, J. P., A. C. Gringarten, A. Menjoz, and P. A. Landel (1982a), Sensi-ble energy-storage in aquifers. 1: Theoretical-study, Water Resour. Res.,18(2), 245–252.

Martin Bloemendal, Niels Hartog, Analysis of the impact of storage conditions on the thermal recovery efficiency of low-temperature ATES systems, Geothermics, Volume 71, 2018, Pages 306-319.

NVOE, 2006. Richtlijnen Ondergrondse Energieopslag, Design Guidelines of Dutch Branche Association for Geothermal Energy Storage. Woerden.

Martin Bloemendal, Theo Olsthoorn, ATES systems in aquifers with high ambient groundwater flow velocity, Geothermics, Volume 75, 2018, Pages 81-92, ISSN 0375-6505.

Masoud Manafi (2022). Role of hydrogeological traits in numerical simulation of aquifer thermal energy storage (Master's thesis, Politecnico di Milano), https://hdl.handle.net/10589/210986.

Krol, M.M., Johnson, R.L., Sleep, B.E., 2014. An analysis of a mixed convection associated with thermal heating in contaminated porous media. Sci. Total Environ. 499, 7–17. https://doi.org/10.1016/j.scitotenv.2014.08.028.

Schout, G., Drijver, B., Gutierrez-Neri, M., Schotting, R., 2014. Analysis of recovery efficiency in high-temperature aquifer thermal energy storage: a Rayleigh-based method. Hydrogeol. J. 22, 281–291. https://doi.org/10.1007/s10040-013-1050-8.

Sheldon, H.A., Wilkins, A., Green, C.P., 2021. Recovery efficiency in high-temperature aquifer thermal energy storage systems. Geothermics. 96, 102173 https://doi.org/ 10.1016/j.geothermics.2021.102173.

Stefan Heldt, Christof Beyer, Sebastian Bauer, Uncertainty assessment of thermal recovery and subsurface temperature changes induced by high-temperature aquifer thermal energy storage (HT-ATES): A case study, Geothermics, Volume 122, 2024, 103086, ISSN 0375-6505.

Felber M., Veronese L., Cocco S., Frei W., Nardin M., Oppizzi P. Santuliana E., Violanti D. (2000) - Indagini sismiche e geologiche nelle valli del Trentino meridionale (Val d'Adige, Valsugana, Valle del Sarca Valle del Chiese). Studi Trentini di Sc. Nat., Acta Geol., Vol. 75 (1998), pp. 3-s2.

Benvenuti G., Dal Prà A., Norinelli A., Piccoli G., Saccardi P. (1970) – Studio idrogeologico della zona del basso Sarca tra Linfano e Riva del Garda. Quad. Ist. Ric. Acque. Ricerche sulle falde acquifere profonde delle vallate alpine ed appenniniche, 6. Roma.

STUDIO GEOLOGICO ASSOCIATO GEOALP, Realizzazione di pozzi di stoccaggio termico in sottosuolo in Comune di Riva del Garda, Trentino, Italia, (2024).

Richards, Lorenzo Adolph. "Capillary conduction of liquids through porous mediums." *physics* 1.5 (1931): 318-333.

Van Genuchten, Martinus & Nielsen, D.R.. (1985). On Describing and Predicting the Hydraulic Properties of Unsaturated Soils. Annales Geophysicae. 3. 615-628.

Doughty, C., Hellström, G., Tsang, C. F., 1982. A Dimensionless Parameter Approach to the Thermal Behavior of an Aquifer Thermal Energy Storage System. Water Resources Research, Vol. 18, No. 3, pages 571-587.

Regnier, G., Salinas, P., Jacquemyn, C., Jackson, M. D., 2022. Numerical Simulation of aquifer thermal energy storage using surface-based geologic modelling and dynamic mesh optimization. Hydrogeology Journal (2022) 30:1179–1198.

Kim, J., Lee, Y., Yoon, W. S., Jeon, J. S., Koo, M. H., Keehm, Y., 2010. Numerical modeling of aquifer thermal energy storage system. Energy 35 (2010) 4955e4965.

Birdsell, D. T., Adams, B. M., Saar, M. O., 2021. Minimum transmissivity and optimal well spacing and flow rate for high-temperature aquifer thermal energy storage. Applied Energy 289 (2021) 116658.

Fleuchaus, P., Godschalk, B., Stober, I., Blum, P., 2018. Worldwide application of aquifer thermal energy storage – A review. Renewable and Sustainable Energy Reviews 94 (2018) 861–876.

Sommer, W., Valstar, J., Van Gaans, P., Grotenhuis, T., Rijnaarts, H., 2013. The impact of aquifer heterogeneity on the performance of aquifer thermal energy storage. Water Resources ResearchVolume 49, Issue 12 p. 8128-8138.

Acknowledgements

The research leading to these results has received funding from the European Union's Horizon Europe research and innovation program under the project USES4HEAT, grant agreement N◦ 101136136. The authors would like to acknowledge the European Commission for the support granted to USES4HEAT.

Funded by the European Union

USES4HEAT